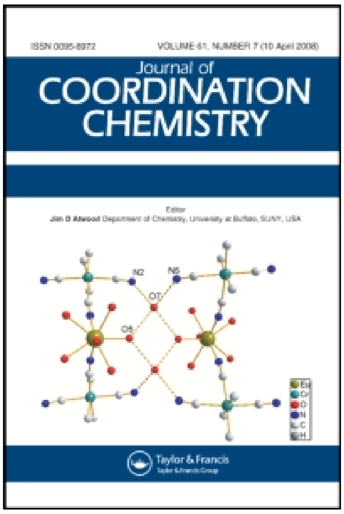

**Journal of Coordination Chemistry**
Publication details, including instructions for authors and subscription information:
http://www.informaworld.com/smpp/title~content=t713455674

# Syntheses, crystal structures, and some properties of heavier lanthanide(III) complexes with optically active *N,N*'-bis(2-hydroxybenzyl)-*N,N*'-bis(2-pyridylmethyl)-*R*-1,2-propanediamine

Yasunori Yamada[a]; Shin-Ichi Takenouchi[a]; Yusuke Miyoshi[a]; Ken-Ichi Okamoto[b]
[a] Faculty of Science and Engineering, Department of Chemistry and Applied Chemistry, Saga University, Saga, Saga 840-8502, Japan [b] Department of Chemistry, Graduate School of Pure and Applied Science, University of Tsukuba, Tsukuba, Ibaraki 305-8571, Japan

**To cite this Article** Yamada, Yasunori , Takenouchi, Shin-Ichi , Miyoshi, Yusuke and Okamoto, Ken-Ichi(2010) 'Syntheses, crystal structures, and some properties of heavier lanthanide(III) complexes with optically active *N,N*'-bis(2-hydroxybenzyl)-*N,N*'-bis(2-pyridylmethyl)-*R*-1,2-propanediamine', Journal of Coordination Chemistry, 63: 6, 996 — 1012

**To link to this Article: DOI:** 10.1080/00958971003682600

**URL:** http://dx.doi.org/10.1080/00958971003682600

*Journal of Coordination Chemistry*
Vol. 63, No. 6, 20 March 2010, 996–1012

# Syntheses, crystal structures, and some properties of heavier lanthanide(III) complexes with optically active *N*,*N*′-bis(2-hydroxybenzyl)-*N*,*N*′-bis(2-pyridylmethyl)-*R*-1,2-propanediamine

YASUNORI YAMADA*†, SHIN-ICHI TAKENOUCHI†,
YUSUKE MIYOSHI† and KEN-ICHI OKAMOTO‡

†Faculty of Science and Engineering, Department of Chemistry and Applied Chemistry,
Saga University, 1 Honjo-machi, Saga, Saga 840-8502, Japan
‡Department of Chemistry, Graduate School of Pure and Applied Science, University of
Tsukuba, 1-1-1 Tennodai, Tsukuba, Ibaraki 305-8571, Japan

(*Received 17 September 2008; in final form 20 November 2009*)

The reaction of *N*,*N*′-bis(2-hydroxybenzyl)-*N*,*N*′-bis(2-pyridylmethyl)-*R*-1,2-propanediamine (*R*-bbppnH$_2$) with Ln(NO$_3$)$_3\cdot n$H$_2$O (Ln = Tb, Dy, Ho, Er, Tm, Yb, or Lu) stereoselectively gave an optically active complex, [Ln(*R*-bbppn)(NO$_3$)]. All the complexes crystallize in the same acentric orthorhombic space group of $C222_1$. The central Ln(III) in the complex is coordinated by four oxygens from two phenolates of *R*-bbppn and one bidentate nitrate and by four nitrogens from two pyridines and one bidentate propanediamine of *R*-bbppn to form a distorted dodecahedral geometry. The combinations of four oxygens and four nitrogens afford two separate trapeziums, which are almost orthogonal to each other. Although two optical isomers, ΔΛΔ and ΛΔΛ, are possible for such a structure, the absolute configuration of the complex is stereoselectively unified to ΔΛΔ. Furthermore, two chiral nitrogens in the complex are fixed to *R* configurations, and the five-membered propanediamine and pyridylmethylamine chelate rings take $\lambda$ and $\delta$ configurations, respectively. These stereoselectivities reflect an introduction of the optically active *R*-propanediamine moiety in the ligand. The electronic absorption, CD, and diffuse reflectance spectra, magnetic susceptibilities, and molar conductivities of the complexes are also discussed in conjunction with their structures.

*Keywords*: Lanthanide(III) complexes; Multidentate ligands; Optically active complexes; Crystal structures; Stereochemistry

## 1. Introduction

The stereochemistry and stereoselectivity of coordination compounds have been developed using chiral organic ligands [1, 2]. In particular, stereoselectivity through the use of optically active diamine chelates has been recognized for the formation of many

---

*Corresponding author. Email: yyamada@cc.saga-u.ac.jp

*Journal of Coordination Chemistry*
ISSN 0095-8972 print/ISSN 1029-0389 online
DOI: 10.1080/00958971003682600

six-coordinated octahedral metal complexes [1]. For some polynuclear, as well as rather simple mononuclear complexes, it has been recognized that the stereoselective constructions can be accomplished with the aid of chiral diamine ligands [3–7]. Concerning higher dimensional coordination polyhedra with lanthanide(III) centers, on the other hand, the stereochemical characteristics attract attention in conjunction with specific physicochemical properties [8–28]. Nevertheless, few attempts have been made at the strategic constructions of complexes with chiral diamine and/or their related polyamine ligands. Such a situation apparently relates to wide variations of possible coordination modes and geometries for the complexes, and hence the use of only simple ligands rarely induces significant stereoselectivities. The use of a multidentate ligand, which is derived from simple diamine, seems to expand the possibilities for structures of the polyhedral lanthanide(III) complexes. Orvig *et al.* [29] operate the controls of structures for some lanthanide(III) complexes using *N*,*N*′-bis(2-hydroxybenzyl)-*N*,*N*′-bis(2-pyridylmethyl)ethylenediamine ($bbpenH_2$), which is derived from ethylenediamine. For instance, the reaction of $bbpenH_2$ with $Yb(NO_3)_3{\cdot}nH_2O$ selectively gave a mononuclear complex, $[Yb(bbpen)(NO_3)]$, eight-coordinate with distorted dodecahedral geometry. Only heavier lanthanide(III) complex, such as $[Yb(bbpen)(NO_3)]$, crystallizes in the acentric space group, $C222_1$, indicating an optically active substance. Taking account of the two possible isomers, ΔΛΔ and ΛΔΛ, for the complex it is no wonder that each optical isomer can be isolated by spontaneous resolution from the reaction solution. It can be considered therefore that the introduction of the chiral diamine moiety into such a hexadentate ligand capacitates stereoselective construction for only one optically active complex. In general, the coordination number of lanthanide(III) in complexes varies from seven to nine. Accordingly, the potentially hexadentate ligand, bbpen, clearly does not satisfy the coordination number requirement of lanthanide(III) ions. In the case of $[Yb(bbpen)(NO_3)]$, however, the eight-coordinate dodecahedral geometry is stabilized by the bidentate nitrate with small bite angle [30–32]. Therefore, the use of nitrate salts of lanthanide(III) is an important factor for the preparations of such complex systems. In this article, we describe syntheses, crystal structures, and some properties of heavier lanthanide(III) complexes with optically active *N*,*N*′-bis(2-hydroxybenzyl)-*N*,*N*′-bis(2-pyridylmethyl)-*R*-1,2-propanediamine (*R*-bbppn), which is derived from *R*-1,2-propanediamine.

## 2. Experimental

### 2.1. *Materials*

$Tb(NO_3)_3 \cdot 6H_2O$, $Dy(NO_3)_3 \cdot 5H_2O$, $Ho(NO_3)_3 \cdot 3H_2O$, $Er(NO_3)_3 \cdot 5H_2O$, $Tm(NO_3)_3 \cdot 4H_2O$, $Yb(NO_3)_3 \cdot 3H_2O$, and $Lu(NO_3)_3 \cdot 3H_2O$ were obtained from Soekawa Chemical Co., Ltd. 1,2-Propanediamine, salicylaldehyde, hexadecyltrimethylammonium bromide, and triethylamine were purchased from Wako Pure Chemical Ind. Co., Ltd. 2-(Chloromethyl)pyridine hydrochloride and potassium borohydride were obtained from Tokyo Chemical Co., Ltd and Merck Co., Ltd, respectively. *N*,*N*′-Bis(2-hydroxybenzyl)-*N*,*N*′-bis(2-pyridylmethyl)-*R*-1,2-propanediamine (*R*-$bbppnH_2$)

was prepared by a similar method to that for bbpen$H_2$ using *N*,*N*′-bis(salicylidene)-*R*-1,2-propanediamine instead of *N*,*N*′-bis(salicylidene)ethylenediamine [29, 33]. The other chemicals were obtained from Wako Pure Chemical Ind. Co., Ltd or Tokyo Chemical Co., Ltd. All the chemicals were of reagent grade and used without purification.

### 2.2. *Preparation of [Tb(R-bbppn)(NO$_3$)]*

*R*-bbppn$H_2$ (0.23 g, 0.5 mmol) was added to a solution containing $Tb(NO_3)_3 \cdot 6H_2O$ (0.23 g, 0.5 mmol) in 30 mL $CH_3CN$. After the mixture was stirred at ambient temperature for 1 h, triethylamine (0.10 g, 1 mmol) was added. The solution was kept at room temperature for several days and the resulting crystals were collected by filtration. Yield: 0.28 g (81% based on Tb). Anal. Calcd for $C_{29}H_{30}N_5O_5Tb$ ([Tb(*R*-bbppn)($NO_3$)]) (%): C, 50.66; H, 4.40; N, 10.19. Found (%): C, 50.68; H, 4.39; N, 10.12. UV-Vis spectrum in $CH_2Cl_2$ [$\nu_{max}$, $10^3\,cm^{-1}$ (log $\epsilon$, $mol^{-1}\,dm^3\,cm^{-1}$)]: 26.3 (−0.2)shoulder(sh), 26.56 (0.10), 27.5 (0.7)sh, 32.9 (3.6)sh, 34.4 (3.9)sh, 36.1 (3.9)sh, 38.0 (4.0)sh, 41.41 (4.36). UV-Vis spectrum in DMF [$\nu_{max}$, $10^3\,cm^{-1}$ (log $\epsilon$, $mol^{-1}\,dm^3\,cm^{-1}$)]: 27.89 (1.03), 33.0 (3.8)sh, 33.90 (3.89), 37.0 (3.9). CD spectrum in $CH_2Cl_2$ [$\nu_{max}$, $10^3\,cm^{-1}$ ($\Delta\epsilon$)]: 26.25 (−3.16), 26.53 (10.19), 26.9 (−4.9)sh, 27.29 (−8.19), 27.6 (−1.0)sh, 33.1 (−10.1)sh, 35.65 (−19.09), 37.95 (16.17), 39.92 (−14.20), 42.46 (39.05). CD spectrum in DMF [$\nu_{max}$, $10^3\,cm^{-1}$ ($\Delta\epsilon$)]: 26.08 (−0.87), 26.28 (−1.26), 26.56 (7.77), 26.92 (−2.44), 27.36 (−2.50), 27.66 (0.23), 27.93 (−1.04), 28.5 (−4.2)sh, 28.7 (−4.7)sh, 31.85 (−0.49), 33.06 (0.82), 35.91 (−5.12). Diffuse reflectance spectrum [$\nu_{max}$, $10^3\,cm^{-1}$]: 31.40, 40.0sh. Molar conductivity in $CH_2Cl_2$ at 296 K [$\Lambda$, $S\,cm^2\,mol^{-1}$]: 0.135. Molar conductivity in DMF at 296 K [$\Lambda$, $S\,cm^2\,mol^{-1}$]: 69.9. Effective magnetic moment at 296 K [$\mu_{eff}$, B.M.]:0 9.38.

### 2.3. *Preparation of [Dy(R-bbppn)(NO$_3$)]*

This complex was prepared by a similar method to that for [Tb(*R*-bbppn)($NO_3$)] using $Dy(NO_3)_3 \cdot 5H_2O$ instead of $Tb(NO_3)_3 \cdot 6H_2O$. Yield: 0.27 g (78% based on Dy). Anal. Calcd for $C_{29}H_{30}N_5O_5Dy$ ([Dy(*R*-bbppn)($NO_3$)]) (%): C, 50.40; H, 4.38; N, 10.14. Found (%): C, 50.43; H, 4.38; N, 10.09. UV-Vis spectrum in $CH_2Cl_2$ [$\nu_{max}$, $10^3\,cm^{-1}$ (log $\epsilon$, $mol^{-1}\,dm^3\,cm^{-1}$)]: 12.61 (−0.37), 12.88 (0.68), 13.33 (−0.56), 13.73 (−0.02), 21.53 (−0.17), 21.81 (−0.26), 22.20 (0.07), 22.45 (0.11), 22.9 (−0.1)sh, 23.67 (−0.18), 25.58 (0.43), 25.77 (0.36), 26.14 (0.39), 26.5 (0.3)sh, 27.0 (0.3)sh, 27.97 (0.96), 29.2 (1.5)sh, 33.7 (3.8)sh, 34.5 (3.9)sh, 37.0 (3.9)sh, 37.7 (4.0)sh, 41.41 (42.24). UV-Vis spectrum in DMF [$\nu_{max}$, $10^3\,cm^{-1}$ (log $\epsilon$, $mol^{-1}\,dm^3\,cm^{-1}$)]: 12.52 (0.10), 12.80 (0.08), 12.89 (0.07), 13.35 (−0.43), 13.63 (−0.51), 13.8 (−0.6)sh, 22.10 (−0.25), 22.20 (−0.18), 22.37 (−0.20), 22.62 (−0.21), 23.64 (−0.30), 25.6 (0.4)sh, 25.71 (0.42), 26.01 (0.31), 26.21 (0.30), 27.6 (0.8)sh, 27.97 (1.02), 33.2 (3.8)sh, 33.90 (3.88), 37.0 (3.9)sh. CD spectrum in $CH_2Cl_2$ [$\nu_{max}$, $10^3\,cm^{-1}$ ($\Delta\epsilon$)]: 12.92 (1.31), 21.51 (−0.37), 21.83 (−2.96), 22.20 (22.13), 22.47 (−6.78), 22.8 (−2.0)sh, 23.73 (1.44), 25.16 (−0.14), 25.87 (4.37), 26.14 (−0.38), 26.32 (0.34), 27.06 (−1.63), 33.0 (−10.0)sh, 35.71 (−19.53), 37.95 (15.05), 39.92 (−14.47), 42.55 (40.37). CD spectrum in DMF [$\nu_{max}$, $10^3\,cm^{-1}$ ($\Delta\epsilon$)]: 12.55 (−1.93), 12.65 (0.56), 12.72 (−1.28), 12.9 (−1.5)sh, 13.00 (−2.81), 13.09 (0.63), 13.23 (0.75), 13.36 (−1.03), 13.50 (0.50), 21.07 (0.51), 21.28 (0.39), 21.55 (0.46), 21.83 (−3.61), 22.17 (18.41), 22.50 (−7.41), 22.70 (−6.61), 23.31 (−0.25), 23.67 (0.97), 25.06 (−0.31), 25.41 (0.99), 25.64 (−1.35), 25.87 (4.64), 26.3 (1.2)sh, 27.21 (−0.84), 27.40 (0.68), 27.66 (−0.68), 27.89 (−0.54), 28.21 (0.85), 28.41 (1.08), 28.57 (1.78), 29.03 (4.07), 29.46 (3.03), 29.54 (2.90), 29.90 (2.81), 30.53 (−6.67), 31.80 (−0.37), 33.06 (1.09), 35.84 (−6.55). Diffuse reflectance spectrum [$\nu_{\max}$, $10^3\,\mathrm{cm}^{-1}$]: 10.72, 10.92, 11.22, 11.56, 12.03, 12.57, 12.90, 13.32, 13.72, 21.51, 21.79, 22.20, 22.42, 22.6sh, 23.67, 25.54, 25.77, 26.11, 26.4sh, 26.99, 27.97, 29.2sh, 33.28, 40.2sh. Molar conductivity in $CH_2Cl_2$ at 296 K [$\Lambda$, $\mathrm{S\,cm^2\,mol^{-1}}$]: 0.050. Molar conductivity in DMF at 296 K [$\Lambda$, $\mathrm{S\,cm^2\,mol^{-1}}$]: 70.4. Effective magnetic moment at 296 K [$\mu_{\mathrm{eff}}$, B.M.]: 10.17.

## 2.4. *Preparation of [Ho(R-bbppn)(NO₃)]*

This complex was prepared by a similar method to that for [Dy(*R*-bbppn)($NO_3$)] using $Ho(NO_3)_3 \cdot 3H_2O$ instead of $Dy(NO_3)_3 \cdot 5H_2O$. Yield: 0.29 g (84% based on Ho). Anal. Calcd for $C_{29}H_{30}N_5O_5Ho$ ([Ho(*R*-bbppn)($NO_3$)]) (%): C, 50.22; H, 4.36; N, 10.10. Found (%): C, 50.22; H, 4.38; N, 10.05. UV-Vis spectrum in $CH_2Cl_2$ [$\nu_{\max}$, $10^3\,\mathrm{cm}^{-1}$ (log $\epsilon$, $\mathrm{mol^{-1}\,dm^3\,cm^{-1}}$)]: 15.2 (0.5)sh, 15.31 (0.55), 15.43 (0.42), 15.54 (0.42), 15.69 (0.40), 18.37 (0.63), 18.62 (0.78), 18.80 (0.38), 20.43 (0.28), 20.62 (0.61), 20.8 (0.1)sh, 21.1 (0.2)sh, 21.25 (0.40), 21.8 (1.2)sh, 21.95 (1.30), 22.05 (1.31), 22.30 (1.02), 23.78 (0.44), 24.04 (0.57), 25.71 (0.08), 25.97 (0.22), 26.28 (0.10), 27.62 (1.13), 32.9 (3.7)sh, 34.4 (3.9)sh, 36.9 (3.9)sh, 37.9 (4.0)sh, 41.41 (4.36). UV-Vis spectrum in DMF [$\nu_{\max}$, $10^3\,\mathrm{cm}^{-1}$ (log $\epsilon$, $\mathrm{mol^{-1}\,dm^3\,cm^{-1}}$)]: 15.34 (0.32), 15.49 (0.45), 15.6 (0.3)sh, 15.87 (−0.16), 18.5 (0.6)sh, 18.57 (0.68), 18.9 (−0.2)sh, 20.58 (0.36), 21.16 (0.19), 21.35 (0.08), 21.7 (0.8)sh, 21.98 (1.10), 22.1 (1.0)sh, 22.5 (0.3)sh, 23.87 (0.49), 24.0 (0.3)sh, 24.39 (−0.27), 25.84 (0.04), 26.11 (0.03), 27.66 (1.02), 32.9 (3.8)sh, 34.01 (3.88), 37.0 (3.9)sh. CD spectrum in $CH_2Cl_2$ [$\nu_{\max}$, $10^3\,\mathrm{cm}^{-1}$ ($\Delta\epsilon$)]: 15.20 (1.73), 15.27 (1.30), 15.40 (−4.48), 15.53 (−4.14), 15.72 (3.80), 18.18 (−1.59), 18.42 (4.06), 18.67 (6.81), 18.85 (−0.70), 20.53 (−0.99), 20.70 (1.25), 21.03 (4.62), 21.30 (−9.10), 21.51 (6.05), 21.74 (11.31), 22.02 (34.76), 22.22 (−1.20), 22.35 (3.59), 23.81 (−2.90), 24.0 (−1.3)sh, 26.04 (−0.72), 26.28 (3.66), 26.7 (0.2)sh, 27.44 (−5.84), 33.1 (−9.9)sh, 35.52 (−18.85), 37.88 (14.71), 39.84 (−14.42), 42.19 (38.99). CD spectrum in DMF [$\nu_{\max}$, $10^3\,\mathrm{cm}^{-1}$ ($\Delta\epsilon$)]: 15.28 (0.26), 15.37 (1.84), 15.49 (1.97), 15.63 (1.38), 15.71 (−2.21), 15.86 (0.80), 15.95 (−2.92), 18.3 (1.1)sh, 18.40 (1.98), 18.59 (−4.89), 18.73 (1.55), 18.83 (−1.57), 18.92 (0.27), 19.03 (−1.15), 20.3 (0.3)sh, 20.45 (0.87), 20.64 (−2.73), 20.96 (1.65), 21.14 (−0.93), 21.44 (6.93), 21.60 (−3.49), 21.76 (3.83), 22.08 (6.75), 22.4 (−0.7)sh, 22.57 (−6.08), 23.42 (−0.16), 23.64 (0.88), 23.84 (−1.13), 24.13 (−0.64), 25.91 (−0.44), 26.0 (−0.4)sh, 26.25 (1.75), 27.17 (0.36), 27.59 (0.62), 27.97 (−1.23), 28.33 (−1.21), 28.9 (−1.7)sh, 31.85 (−0.65), 33.11 (0.85), 35.91 (−4.44). Diffuse reflectance spectrum [$\nu_{\max}$, $10^3\,\mathrm{cm}^{-1}$]: 11.29, 15.2sh, 15.30, 15.43, 15.52, 15.66, 18.37, 18.59, 18.78, 20.43, 20.60, 20.8sh, 20.9sh, 21.23, 21.7sh, 21.95, 22.05, 22.27, 23.78, 24.01, 25.7sh, 25.94, 26.2sh, 27.59, 33.06, 40.1sh. Molar conductivity in $CH_2Cl_2$ at 296 K [$\Lambda$, $\mathrm{S\,cm^2\,mol^{-1}}$]: 0.050. Molar conductivity in DMF at 296 K [$\Lambda$, $\mathrm{S\,cm^2\,mol^{-1}}$]: 69.8. Effective magnetic moment at 296 K [$\mu_{\mathrm{eff}}$, B.M.]: 10.31.

## 2.5. *Preparation of [Er(R-bbppn)(NO$_3$)]*

This complex was prepared by a similar method to that for [Ho(*R*-bbppn)(NO$_3$)] using $Er(NO_3)_3 \cdot 5H_2O$ instead of $Ho(NO_3)_3 \cdot 3H_2O$. Yield: 0.26 g (75% based on Er). Anal. Calcd for $C_{29}H_{30}N_5O_5Er$ ([Er(*R*-bbppn)(NO$_3$)]) (%): C, 50.05; H, 4.34; N, 10.07. Found (%): C, 50.09; H, 4.35; N, 10.00. UV-Vis spectrum in $CH_2Cl_2$ [$\nu_{max}$, $10^3\,cm^{-1}$ (log $\epsilon$, $mol^{-1}\,dm^3\,cm^{-1}$)]: 12.54 (−0.43), 14.9 (−0.6)sh, 15.1 (0.2)sh, 15.18 (0.43), 15.40 (0.01), 18.2 (−0.2)sh, 18.32 (0.02), 18.42 (0.01), 18.6 (−0.3)sh, 19.2 (1.2)sh, 19.21 (1.43), 20.31 (0.55), 20.4 (0.3)sh, 22.0 (0.1)sh, 22.12 (0.06), 22.60 (−0.35), 24.54 (0.13), 25.5 (−0.5)sh, 26.42 (1.63), 27.40 (0.90), 28.1 (0.9)sh, 33.4 (3.8)sh, 34.4 (3.6)sh, 36.9 (3.9)sh, 37.8 (4.0)sh, 41.49 (4.36). UV-Vis spectrum in DMF [$\nu_{max}$, $10^3\,cm^{-1}$ (log $\epsilon$, $mol^{-1}\,dm^3\,cm^{-1}$)]: 12.52 (−0.48), 12.58 (−0.48), 14.9 (−0.4)sh, 15.1 (0.2)sh, 15.22 (0.35), 15.3 (0.2)sh, 18.2 (−0.3)sh, 18.38 (−0.01), 18.45 (0.02), 19.1 (0.9)sh, 19.23 (1.05), 20.37 (0.41), 20.5 (0.3)sh, 22.0 (−0.2)sh, 22.17 (0.08), 22.55 (−0.26), 24.54 (0.16), 26.46 (1.35), 27.40 (0.81), 28.0 (1.0)sh, 32.9 (3.8)sh, 33.84 (3.88), 36.9 (3.9)sh. CD spectrum in $CH_2Cl_2$ [$\nu_{max}$, $10^3\,cm^{-1}$ ($\Delta\epsilon$)]: 12.78 (0.61), 15.14 (−1.19), 15.26 (1.20), 15.39 (1.65), 15.54 (−0.99), 18.37 (0.71), 18.50 (−0.96), 19.01 (8.68), 19.27 (17.20), 20.26 (−0.37), 20.43 (0.65), 20.62 (−2.04), 24.72 (0.66), 25.87 (−0.80), 26.42 (10.03), 27.0 (−1.0)sh, 27.17 (−1.38), 27.51 (6.48), 28.0 (−8.3)sh, 32.8 (−9.2)sh, 35.52 (−18.83), 37.88 (13.72), 39.84 (−14.36), 42.46 (38.19). CD spectrum in DMF [$\nu_{max}$, $10^3\,cm^{-1}$ ($\Delta\epsilon$)]: 12.61 (2.33), 12.68 (−1.38), 12.77 (−1.17), 12.80 (−1.27), 15.23 (2.88), 15.36 (−2.43), 15.44 (0.25), 15.53 (−1.16), 18.3 (0.9)sh, 18.37 (1.89), 18.55 (1.48), 19.0 (2.4)sh, 19.27 (6.59), 19.42 (−0.46), 20.28 (−0.36), 20.43 (1.72), 20.70 (2.00), 22.00 (0.60), 22.15 (0.67), 22.47 (0.46), 22.75 (0.15), 24.33 (0.31), 24.72 (1.01), 25.84 (−0.49), 26.49 (9.28), 26.95 (−0.11), 27.25 (−2.32), 27.51 (4.38), 27.86 (−4.27), 31.85 (−0.73), 33.06 (0.75), 35.91 (−4.16). Diffuse reflectance spectrum [$\nu_{max}$, $10^3\,cm^{-1}$]: 10.23, 10.40, 12.09, 12.30, 12.46, 12.53, 14.66, 14.7sh, 15.18, 15.39, 17.78, 18.2sh, 18.32, 18.4sh, 18.5sh, 19.1sh, 19.21, 20.28, 20.4sh, 22.0sh, 22.10, 22.55, 24.51, 25.7sh, 26.42, 27.36, 28.0sh, 33.9sh, 40.9sh. Molar conductivity in $CH_2Cl_2$ at 296 K [$\Lambda$, $S\,cm^2\,mol^{-1}$]: 0.070. Molar conductivity in DMF at 296 K [$\Lambda$, $S\,cm^2\,mol^{-1}$]: 66.2. Effective magnetic moment at 296 K [$\mu_{eff}$, B.M.]: 9.14.

## 2.6. *Preparation of [Tm(R-bbppn)(NO$_3$)]*

This complex was prepared by a similar method to that for [Er(*R*-bbppn)(NO$_3$)] using $Tm(NO_3)_3 \cdot 4H_2O$ instead of $Er(NO_3)_3 \cdot 5H_2O$. Yield: 0.25 g (71% based on Tm). Anal. Calcd for $C_{29}H_{30}N_5O_5Tm$ ([Tm(*R*-bbppn)(NO$_3$)]) (%): C, 49.93; H, 4.34; N, 10.04. Found (%): C, 49.92; H, 4.37; N, 9.98. UV-Vis spectrum in $CH_2Cl_2$ [$\nu_{max}$, $10^3\,cm^{-1}$ (log $\epsilon$, $mol^{-1}\,dm^3\,cm^{-1}$)]: 12.57 (1.29), 13.03 (−0.14), 13.99 (−0.69), 14.4 (0.3)sh, 14.5 (0.6)sh, 14.61 (0.71), 14.89 (0.23), 15.36 (−0.31), 21.3 (0.3)sh, 21.41 (0.48), 27.6 (0.6)sh, 28.13 (1.40), 33.5 (3.8)sh, 34.4 (3.9)sh, 36.8 (3.9)sh, 37.8 (4.0)sh, 41.49 (4.34). UV-Vis spectrum in DMF [$\nu_{max}$, $10^3\,cm^{-1}$ (log $\epsilon$, $mol^{-1}\,dm^3\,cm^{-1}$)]: 12.57 (0.84), 12.8 (0.1)sh, 14.54 (0.57), 14.90 (0.02), 15.27 (−0.46), 21.3 (0.1)sh, 21.41 (0.14), 28.1 (1.1)sh, 33.3 (3.8)sh, 33.96 (3.88), 37.0 (3.9)sh. CD spectrum in $CH_2Cl_2$ [$\nu_{max}$, $10^3\,cm^{-1}$ ($\Delta\epsilon$)]: 12.52 (−2.94), 12.63 (65.47), 13.00 (3.51), 13.18 (3.34), 13.30 (1.85), 13.49 (2.37), 14.36 (3.37), 14.49 (6.94), 14.61 (−14.08), 14.78 (−6.81), 14.99 (4.25), 15.70 (2.09), 21.14 (2.85), 21.46 (5.21), 32.8 (−8.9)sh, 35.59 (−18.49), 37.88 (12.50), 39.84 (−12.10), 42.55 (36.31). CD spectrum in DMF [$\nu_{max}$, $10^3\,cm^{-1}$ ($\Delta\epsilon$)]: 12.53 (−6.60), 12.63 (23.66), 12.85 (4.81), 12.9 (3.5)sh, 13.1 (5.6)sh, 13.10 (5.90), 13.23 (1.34), 13.51 (1.10), 13.69 (1.07), 14.07 (0.80), 14.24 (−0.59), 14.3 (0.7)sh, 14.51 (12.76), 14.70 (11.55), 14.9 (1.9)sh, 14.99 (3.51), 15.21 (3.48), 15.63 (0.60), 21.14 (1.47), 21.51 (2.48), 27.55 (−4.11), 28.09 (5.98), 28.57 (3.46), 28.78 (1.76), 29.11 (−0.88), 29.6 (−6.2)sh, 31.20 (−0.25), 33.06 (1.11), 35.91 (−4.59). Diffuse reflectance spectrum [$\nu_{max}$, $10^3\,cm^{-1}$]: 12.57, 13.03, 13.86, 14.4sh, 14.5sh, 14.62, 14.89, 15.36, 21.1sh, 21.41, 27.4sh, 28.13, 33.33, 41.0sh. Molar conductivity in $CH_2Cl_2$ at 296 K [$\Lambda$, $S\,cm^2\,mol^{-1}$]: 0.030. Molar conductivity in DMF at 296 K [$\Lambda$, $S\,cm^2\,mol^{-1}$]: 69.8. Effective magnetic moment at 296 K [$\mu_{eff}$, B.M.]: 7.26.

### 2.7. *Preparation of [Yb(R-bbppn)(NO₃)]*

This complex was prepared by a similar method to that for [Tm(*R*-bbppn)($NO_3$)] using $Yb(NO_3)_3 \cdot 3H_2O$ instead of $Tm(NO_3)_3 \cdot 4H_2O$. Yield: 0.26 g (74% based on Yb). Anal. Calcd for $C_{29}H_{30}N_5O_5Yb$ ([Yb(*R*-bbppn)($NO_3$)]) (%): C, 49.64; H, 4.31; N, 9.98%. Found (%): C, 49.65; H, 4.30; N, 9.93. UV-Vis spectrum in $CH_2Cl_2$ [$\nu_{max}$, $10^3\,cm^{-1}$ (log $\epsilon$, $mol^{-1}\,dm^3\,cm^{-1}$)]: 27.2 (2.1)sh, 33.4 (3.8)sh, 34.42 (3.85), 36.2 (3.8)sh, 37.7 (4.0)sh, 41.58 (4.34). UV-Vis spectrum in DMF [$\nu_{max}$, $10^3\,cm^{-1}$ (log $\epsilon$, $mol^{-1}\,dm^3\,cm^{-1}$)]: 27.2 (2.1)sh, 33.0 (3.8)sh, 33.96 (3.88), 37.1 (3.9)sh. CD spectrum in $CH_2Cl_2$ [$\nu_{max}$, $10^3\,cm^{-1}$ ($\Delta\epsilon$)]: 27.21 (4.12), 32.7 (−7.8)sh, 35.71 (−18.80), 37.95 (10.88), 40.00 (−13.35), 42.64 (34.83). CD spectrum in DMF [$\nu_{max}$, $10^3\,cm^{-1}$ ($\Delta\epsilon$)]: 29.41 (5.87), 29.50 (6.17), 29.6 (7.3)sh, 29.76 (10.46), 29.90 (12.23), 30.35 (10.88), 30.44 (11.16), 30.6 (9.6)sh, 30.8 (10.4)sh, 30.9 (11.8)sh, 31.01 (12.52), 31.25, (9.88), 31.4 (9.7)sh, 31.50 (10.60), 33.17 (2.42), 35.97 (−5.16). Diffuse reflectance spectrum [$\nu_{max}$, $10^3\,cm^{-1}$]: 10.1sh, 10.21, 10.42, 10.78, 27.3sh, 32.89, 41.8sh. Molar conductivity in $CH_2Cl_2$ at 296 K [$\Lambda$, $S\,cm^2\,mol^{-1}$]: 0.060. Molar conductivity in DMF at 296 K [$\Lambda$, $S\,cm^2\,mol^{-1}$]: 69.8. Effective magnetic moment at 296 K [$\mu_{eff}$, B.M.]: 4.42.

### 2.8. *Preparation of [Lu(R-bbppn)(NO₃)]*

This complex was prepared by a similar method to that for [Yb(*R*-bbppn)($NO_3$)] using $Lu(NO_3)_3 \cdot 3H_2O$ instead of $Yb(NO_3)_3 \cdot 3H_2O$. Yield: 0.28 g (80% based on Lu). Anal. Calcd for $C_{29}H_{30}N_5O_5Lu$ ([Lu(*R*-bbppn)($NO_3$)]) (%): C, 49.50; H, 4.30; N, 9.96. Found (%): C, 49.50; H, 4.34; N, 9.88. UV-Vis spectrum in $CH_2Cl_2$ [$\nu_{max}$, $10^3\,cm^{-1}$ (log $\epsilon$, $mol^{-1}\,dm^3\,cm^{-1}$)]: 33.0 (3.7)sh, 34.42 (3.86), 36.8 (3.9)sh, 38.0 (4.0)sh, 41.49 (4.35). UV-Vis spectrum in DMF [$\nu_{max}$, $10^3\,cm^{-1}$ (log $\epsilon$, $mol^{-1}\,dm^3\,cm^{-1}$)]: 33.0 (3.8)sh, 33.84 (3.87), 36.9 (3.9)sh. CD spectrum in $CH_2Cl_2$ [$\nu_{max}$, $10^3\,cm^{-1}$ ($\Delta\epsilon$)]: 32.6 (−7.7)sh, 35.46 (−18.33), 37.88 (11.62), 39.84 (−13.84), 42.46 (35.14). CD spectrum in DMF [$\nu_{max}$, $10^3\,cm^{-1}$ ($\Delta\epsilon$)]: 27.36 (−1.18), 27.82 (0.88), 31.85 (−0.70), 33.17 (0.88), 35.91 (−4.23). Diffuse reflectance spectrum [$\nu_{max}$, $10^3\,cm^{-1}$]: 33.00, 41.4sh. Molar conductivity in $CH_2Cl_2$ at 296 K [$\Lambda$, $S\,cm^2\,mol^{-1}$]: 0.030. Molar conductivity in DMF at 296 K [$\Lambda$, $S\,cm^2\,mol^{-1}$]: 69.5. Effective magnetic moment at 296 K [$\mu_{eff}$, B.M.]: 0.07. $^1H$ NMR (300 MHz, $CDCl_3$), $\delta = 0.94$ (d, 3H, methyl), 2.27 (dd, 1H, methylene), 2.64 (t, 1H, methylene), 2.78 (d, 1H, methylene), 2.86–2.98 (m, 1H, methine), 3.13 (d, 1H, methylene), 3.46 (d, 1H, methylene), 3.70 (d, 1H, methylene), 3.83 (d, 1H, methylene), 4.11 (d, 1H, methylene), 4.41 (d, 1H, methylene), 4.69 (d, 1H, methylene), 6.39–6.48 (m, 4H, phenyl), 6.82–6.89 (m, 2H, phenyl), 7.04–7.11 (m, 2H, phenyl), 7.30–7.44 (m, 4H, pyridyl), 7.86 (td, 2H, pyridyl), 8.66 (t, 2H, pyridyl).

### 2.9. *Measurements*

The electronic absorption spectra were recorded with a Perkin-Elmer Lambda 19 spectrophotometer, and the CD spectra with a JASCO J-600 spectropolarimeter. The diffuse reflectance spectra were measured with a JASCO Ubest V-570 spectrophotometer equipped with an integrating sphere apparatus. Magnetic measurements were performed using a Sherwood Scientific susceptibility apparatus at 23°C. Diamagnetic corrections employed tabulated constants [34]. The molar conductances of the complexes were measured with a TOA CM-30G conductivity meter in $CH_2Cl_2$ and DMF solution at 23°C. Elemental analyses (C, H, N) were performed with a Perkin-Elmer 2400 CHN Elemental Analyzer. The $^1H$ NMR spectra were recorded with a JEOL JNM-AL300 NMR spectrometer in $CDCl_3$ using tetramethylsilane (THF) as an internal reference. The solid state photoluminescence spectrum of [Ln(*R*-bbppn)($NO_3$)] was measured with an OceanOptics USB4000-FL fluorescence spectrometer equipped with a DH-2000-BAL balanced deuterium tungsten halogen light source.

### 2.10. *X-ray structure determination*

Single crystals of [Ln(*R*-bbppn)($NO_3$)] (Ln = Tb, Dy, Ho, Er, Tm, Yb, Lu) were used for the data collection on a Rigaku RASA-7S four-circle diffractometer with graphite-monochromated Mo-K$\alpha$ ($\lambda = 0.71069$ Å) radiation. Cell constants and an orientation matrix for the data collection were obtained from a least-squares refinement using the setting angles of 25 carefully centered reflections in the range $14° < \theta < 15°$. The data were collected at $296 \pm 1$ K using the $\omega$–$2\theta$ scan technique to a maximum $2\theta$ value of 55°. The weak reflections ($I < 10.0\sigma(I)$) were rescanned (maximum of five scans) and the counts were accumulated to ensure the good counting statistics. The stationary background counts were recorded on each side of the reflection. The ratio of peak counting time to background counting time was 2: 1. The intensities of three representative reflections were measured after every 150 reflections. Over the course of data collection, the standards decreased by 0.0–1.4%. The polynomial correction factors were applied to the data to account for this phenomenon. The empirical absorption corrections based on the azimuthal scans of several reflections were applied. The data were corrected for Lorentz and polarization effects. The crystal data and experimental parameters are summarized in table 1.

The structures were solved by heavy-atom Patterson methods and expanded using Fourier techniques [35, 36]. The non-hydrogen atoms were refined anisotropically. All hydrogens were refined using the riding model. The final cycle of full-matrix least-squares refinement on $F$ was based on the observed reflections ($I > 2.00\sigma(I)$) and variable parameters, and converged with the unweighted and weighted agreement factors of $R$ and $R_w$. The neutral atom scattering factors were taken from Cromer and

Table 1. Crystallographic data for [Ln(*R*-bbppn)($NO_3$)] (Ln = Tb, Dy, Ho, Er, Tm, Yb, Lu).

| | [Tb(*R*-bbppn) ($NO_3$)] | [Dy(*R*-bbppn) ($NO_3$)] | [Ho(*R*-bbppn) ($NO_3$)] | [Er(*R*-bbppn) ($NO_3$)]O | [Tm(*R*-bbppn) ($NO_3$)] | [Yb(*R*-bbppn) ($NO_3$)] | [Lu(*R*-bbppn) ($NO_3$)] |
|---|---|---|---|---|---|---|---|
| Emperical formula | $C_{29}H_{30}N_5O_5Tb$ | $C_{29}H_{30}N_5O_5Dy$ | $C_{29}H_{30}N_5O_5Ho$ | $C_{29}H_{30}N_5O_5Er$ | $C_{29}H_{30}N_5O_5Tm$ | $C_{29}H_{30}N_5O_5Yb$ | $C_{29}H_{30}N_5O_5Lu$ |
| Formula weight | 687.51 | 691.09 | 693.52 | 695.85 | 697.52 | 701.63 | 703.55 |
| Crystal size ($mm^3$) | 0.08 × 0.25 × 0.40 | 0.10 × 0.35 × 0.43 | 0.10 × 0.20 × 0.20 | 0.10 × 0.20 × 0.20 | 0.10 × 0.34 × 0.40 | 0.10 × 0.15 × 0.30 | 0.15 × 0.30 × 0.65 |
| Space group | *C222₁* | *C222₁* | *C222₁* | *C222₁* | *C222₁* | *C222₁* | *C222₁* |
| Unit cell dimensions (Å, °) | | | | | | | |
| *a* | 8.711(2) | 8.698(4) | 8.674(3) | 8.657(2) | 8.653(1) | 8.636(3) | 8.625(1) |
| *b* | 19.09(1) | 19.12(2) | 19.071(10) | 19.06(1) | 19.072(6) | 19.039(8) | 19.061(4) |
| *c* | 16.977(3) | 17.021(7) | 16.969(5) | 16.942(7) | 16.969(3) | 16.952(5) | 16.948(2) |
| $\alpha$ | 90 | 90 | 90 | 90 | 90 | 90 | 90 |
| $\beta$ | 90 | 90 | 90 | 90 | 90 | 90 | 90 |
| $\gamma$ | 90 | 90 | 90 | 90 | 90 | 90 | 90 |
| Volume (Å$^3$), *Z* | 2822(1), 4 | 2830(3), 4 | 2806(1), 4 | 2796(2), 4 | 2800(1), 4 | 2787(1), 4 | 2786.4(9), 4 |
| Calculated density ($g\,cm^{-3}$) | 1.618 | 1.622 | 1.641 | 1.653 | 1.654 | 1.672 | 1.677 |
| Absorption coefficient ($cm^{-1}$) | 25.47 | 26.91 | 28.70 | 30.43 | 32.08 | 34.03 | 35.91 |
| Transition factors | 0.72–1.00 | 0.70–1.00 | 0.74–1.00 | 0.78–1.00 | 0.68–1.00 | 0.76–1.00 | 0.60–1.00 |
| Total reflections | 1908 | 1919 | 1902 | 1899 | 1900 | 1892 | 1888 |
| Reflection ($I > 2\sigma(I)$) | 1543 | 1603 | 1590 | 1558 | 1657 | 1505 | 1667 |
| No. of variables | 187 | 187 | 187 | 187 | 187 | 187 | 187 |
| $R$ ($R_w$) | 0.033 (0.041) | 0.033 (0.045) | 0.032 (0.041) | 0.034 (0.044) | 0.026 (0.036) | 0.038 (0.046) | 0.020 (0.028) |
| Goodness-of-fit on $F^2$ | 1.07 | 1.22 | 1.03 | 1.09 | 1.02 | 1.16 | 0.90 |

Waber [37]. The anomalous dispersion effects were included in $F_c$; the values for $\Delta f'$ and $\Delta f''$ were those of Creagh and McAuley [38, 39]. The values for the mass attenuation coefficients are those of Creagh and Hubbell [40]. The absolute configurations for the complexes were determined on the basis of the known *R* configuration of the asymmetric carbon atom in *R*-pn framework, and the structures were supported by the Flack parameters (0.05(2) for [Tb(*R*-bbppn)($NO_3$)], 0.03(2) for [Dy(*R*-bbppn)($NO_3$)], 0.04(2) for [Ho(*R*-bbppn)($NO_3$)], 0.01(2) for [Er(*R*-bbppn)($NO_3$)], 0.00(1) for [Tm(*R*-bbppn)($NO_3$)], 0.00(2) for [Yb(*R*-bbppn)($NO_3$)], and 0.05(1) for [Lu(*R*-bbppn)($NO_3$)]) [41]. All calculations were performed using the teXsan crystallographic software package of Molecular Structure Corporation [42].

## 3. Results and discussion

### 3.1. *Crystal structures*

All the lanthanide(III) complexes, [Ln(*R*-bbppn)($NO_3$)] (Ln = Tb, Dy, Ho, Er, Tm, Yb, Lu), crystallize in the same acentric orthorhombic space group of *C222₁* (table 1). A perspective drawing of [Er(*R*-bbppn)($NO_3$)] is shown in figure 1 as a typical example

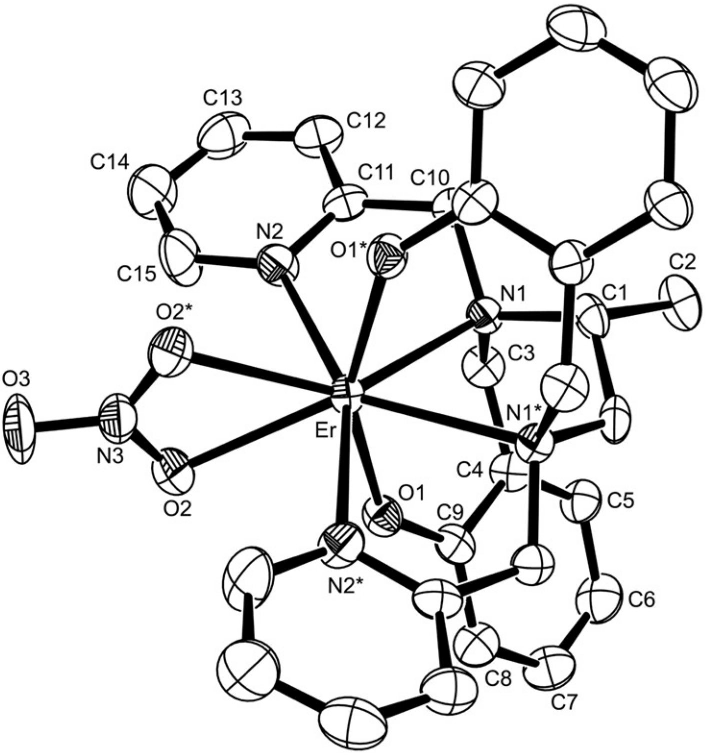

Figure 1. Perspective view of [Er(*R*-bbppn)($NO_3$)] with the atomic labeling scheme (30% probability ellipsoids). Symmetry codes for the atoms with *: $2 - x$, $y$, $3/2 - z$.

of [Ln(*R*-bbppn)($NO_3$)]. An X-ray structural analysis for [Er(*R*-bbppn)($NO_3$)] revealed that the central Er(III) adopts eight-coordination with distorted dodecahedral geometry. In [Er(*R*-bbppn)($NO_3$)], the four coordinated oxygens are in almost the same plane (dihedral angle between ErO1O1* and ErO2O2*: 7.2°) to afford a trapezium in which the O1 and O1* of *R*-bbppn lie on the lower base and the O2 and O2* of nitrate locate on the upper base. Another trapezium is established by the remaining four coordinated nitrogens of *R*-bbppn in which N1 and N1* are situated on the lower base and the N2 and N2* are on the upper base. These two trapezoid bodies are almost orthogonal to each other, forming a distorted dodecahedron. The ligand *R*-bbppn in the complex possesses six coordination sites to form five chelate rings, three five-membered ErN1C1C1*N1*, ErN1C10C11N2, and ErN1*C10*C11*N2* chelate rings, and two six-membered ErN1C3C4C9O1 and ErN1*C3*C4*C9*O1* chelate rings. Among these five chelate rings, the three pairs ErN1C10C11N2–ErN1*C3*C4*C9*O1*, ErN1C3C4C9O1–ErN1*C3*C4*C9*O1*, and ErN1C3C4C9O1–ErN1*C10*C11*N2* are valid for the determination of absolute configuration of the complex [43]. The ErN1C10C11N2–ErN1*C3*C4*C9*O1*, ErN1C3C4C9O1–ErN1*C3*C4*C9*O1*, and ErN1C3C4C9O1–ErN1*C10*C11*N2* pairs afford Δ, Λ, and Δ configurations, respectively, and hence the absolute configuration of the complex is ΔΛΔ. Although two isomers (ΔΛΔ and ΛΔΛ) are possible for the complex, the absolute configuration of the complex is stereoselectively unified to ΔΛΔ. Furthermore, two chiral nitrogens in the complex, N1 and N1*, are fixed to *R* configurations. In addition, the five-membered propanediamine chelate ring takes $\lambda$ configuration, while two five-membered pyridylmethylamine chelate rings acquire $\delta$ configurations. Such stereoselectivity is also observed for the remaining complexes, [Ln(*R*-bbppn)($NO_3$)] (Ln = Tb, Dy, Ho, Tm, Yb, Lu). Although a similar ΛΔΛ isomer was incidentally obtained by spontaneous resolution from the solution of the racemic (ΔΛΔ and ΛΔΛ) mixture of [Yb(bbpen)($NO_3$)], no stereoselectivity occurs in the complex [29]. It can be concluded therefore that the above stereoselectivity for [Ln(*R*-bbppn)($NO_3$)] is derived from the optically active *R*-propanediamine moiety in *R*-bbppn. As shown in table 2, all the bond distances between Er(III) and coordinated atoms are shorter than the corresponding distances in [Ho(*R*-bbppn)($NO_3$)], but are longer than those in [Tm(*R*-bbppn)($NO_3$)]. This suggests that the bond distance decreases with an increase in the atomic number. It can be actually confirmed by the plots of bond distances against atomic numbers of the complexes (figure 2). This reflects the lanthanide contraction in the present Ln(III) complexes.

### 3.2. *Characterization*

The effective magnetic moments ($\mu_{eff}$) at 296 K were 9.38 B.M. for [Tb(*R*-bbppn)($NO_3$)], 10.17 B.M. for [Dy(*R*-bbppn)($NO_3$)], 10.31 B.M. for [Ho(*R*-bbppn)($NO_3$)], 9.14 B.M. for [Er(*R*-bbppn)($NO_3$)], 7.26 B.M. for [Tm(*R*-bbppn)($NO_3$)], 4.42 B.M. for [Yb(*R*-bbppn)($NO_3$)], and 0.06 B.M. for [Lu(*R*-bbppn)($NO_3$)]. These observed values

Table 2. Selected bond distances (Å) and angles (°) for [Ln(*R*-bbppn)($NO_3$)] (Ln = Tb, Dy, Ho, Er, Tm, Yb, Lu).

| | Tb | Dy | Ho | Er | Tm | Yb | Lu |
|---|---|---|---|---|---|---|---|
| Ln–O1 | 2.192(4) | 2.172(4) | 2.179(4) | 2.164(5) | 2.152(3) | 2.158(6) | 2.143(3) |
| Ln–O1$^a$ | 2.192(4) | 2.172(4) | 2.179(4) | 2.164(5) | 2.152(3) | 2.158(6) | 2.143(3) |
| Ln–O2 | 2.486(5) | 2.493(5) | 2.464(5) | 2.458(6) | 2.450(4) | 2.442(6) | 2.428(3) |
| Ln–O2$^a$ | 2.486(5) | 2.493(5) | 2.464(5) | 2.458(6) | 2.450(4) | 2.442(6) | 2.428(3) |
| Ln–N1 | 2.588(5) | 2.581(5) | 2.565(5) | 2.550(6) | 2.541(4) | 2.521(7) | 2.523(3) |
| Ln–N1$^a$ | 2.588(5) | 2.581(5) | 2.565(5) | 2.550(6) | 2.541(4) | 2.521(7) | 2.523(3) |
| Ln–N2 | 2.546(6) | 2.544(6) | 2.538(6) | 2.522(6) | 2.518(5) | 2.491(8) | 2.493(4) |
| Ln–N2$^a$ | 2.546(6) | 2.544(6) | 2.538(6) | 2.522(6) | 2.518(5) | 2.491(8) | 2.493(4) |
| O1–Ln–O1$^a$ | 153.2(2) | 154.6(2) | 153.8(2) | 154.3(3) | 154.9(2) | 154.7(3) | 155.5(2) |
| O1–Ln–O2 | 77.9(2) | 77.7(2) | 77.5(2) | 76.8(2) | 76.7(2) | 76.2(2) | 76.2(1) |
| O1–Ln–O2$^a$ | 128.9(2) | 127.6(2) | 128.7(2) | 128.9(2) | 128.3(2) | 129.0(2) | 128.3(1) |
| O1–Ln–N1 | 75.6(2) | 76.7(2) | 76.0(2) | 76.3(2) | 77.0(1) | 76.6(2) | 77.2(1) |
| O1–Ln–N1$^a$ | 82.5(2) | 82.7(2) | 82.6(2) | 82.8(2) | 82.7(1) | 82.9(2) | 82.9(1) |
| O1–Ln–N2 | 98.3(2) | 98.2(2) | 98.4(2) | 98.1(2) | 98.5(2) | 97.8(2) | 98.5(1) |
| O1–Ln–N2$^a$ | 86.7(2) | 86.7(2) | 86.8(2) | 86.9(2) | 86.4(2) | 87.5(2) | 86.6(1) |
| O1$^a$–Ln–O2 | 128.9(2) | 127.6(2) | 128.7(2) | 128.9(2) | 128.3(2) | 129.0(2) | 128.3(1) |
| O1$^a$–Ln–O2$^a$ | 77.9(2) | 77.7(2) | 77.5(2) | 76.8(2) | 76.7(2) | 76.2(2) | 76.2(1) |
| O1$^a$–Ln–N1 | 82.5(2) | 82.7(2) | 82.6(2) | 82.8(2) | 82.7(1) | 82.9(2) | 82.9(1) |
| O1$^a$–Ln–N1$^a$ | 75.6(2) | 76.7(2) | 76.0(2) | 76.3(2) | 77.0(1) | 76.6(2) | 77.2(1) |
| O1$^a$–Ln–N2 | 86.7(2) | 86.7(2) | 86.8(2) | 86.9(2) | 86.4(2) | 87.5(2) | 86.6(1) |
| O1$^a$–Ln–N2$^a$ | 98.3(2) | 98.2(2) | 98.4(2) | 98.1(2) | 98.5(2) | 97.8(2) | 98.5(1) |
| O2–Ln–O2$^a$ | 51.4(3) | 50.4(3) | 51.7(3) | 52.5(3) | 52.1(2) | 53.1(3) | 52.4(2) |
| O2–Ln–N1 | 132.7(2) | 132.9(2) | 132.7(2) | 132.3(2) | 132.4(1) | 132.5(2) | 132.7(1) |
| O2–Ln–N1$^a$ | 142.4(2) | 142.5(2) | 142.4(2) | 141.9(2) | 141.6(2) | 141.3(2) | 141.3(1) |
| O2–Ln–N2 | 79.9(2) | 79.1(2) | 79.1(2) | 79.3(2) | 79.3(2) | 78.9(3) | 79.2(1) |
| O2–Ln–N2$^a$ | 80.8(2) | 80.8(2) | 80.2(2) | 80.4(2) | 80.3(2) | 79.6(3) | 79.4(1) |
| O2$^a$–Ln–N1 | 142.4(2) | 142.5(2) | 142.4(2) | 141.9(2) | 141.6(2) | 141.3(2) | 141.3(1) |
| O2$^a$–Ln–N1$^a$ | 132.7(2) | 132.9(2) | 132.7(2) | 132.3(2) | 132.4(1) | 132.5(2) | 132.7(1) |
| O2$^a$–Ln–N2 | 80.8(2) | 80.8(2) | 80.2(2) | 80.4(2) | 80.3(2) | 79.6(3) | 79.4(1) |
| O2$^a$–Ln–N2$^a$ | 79.9(2) | 79.1(2) | 79.1(2) | 79.3(2) | 79.3(2) | 78.9(3) | 79.2(1) |
| N1–Ln–N1$^a$ | 70.7(2) | 71.0(2) | 70.4(2) | 71.0(2) | 71.6(2) | 71.1(3) | 71.1(1) |
| N1–Ln–N2 | 66.2(2) | 66.3(2) | 67.1(2) | 66.6(2) | 66.3(2) | 67.1(3) | 67.1(1) |
| N1–Ln–N2$^a$ | 135.0(2) | 135.7(2) | 135.8(2) | 135.9(2) | 136.2(2) | 136.7(3) | 136.6(1) |
| N1$^a$–Ln–N2 | 135.0(2) | 135.7(2) | 135.8(2) | 135.9(2) | 136.2(2) | 136.7(3) | 136.6(1) |
| N1$^a$–Ln–N2$^a$ | 66.2(2) | 66.3(2) | 67.1(2) | 66.6(2) | 66.3(2) | 67.1(3) | 67.1(1) |
| N2–Ln–N2$^a$ | 158.6(3) | 157.7(3) | 156.9(3) | 157.3(3) | 157.3(2) | 155.9(4) | 156.1(2) |

Symmetry codes for the atoms with a: $2-x$, $y$, $3/2-z$.

correspond well with the calculated ones based on Hund's rule. This indicates the shielded f orbitals in [Ln(*R*-bbppn)($NO_3$)].

Among these seven complexes, the antiferromagnetic Lu complex affords $^1H$ NMR spectrum in $CDCl_3$. In $CDCl_3$, [Lu(*R*-bbppn)($NO_3$)] shows $^1H$ NMR signals due to the saturated and unsaturated hydrocarbons in the higher and lower magnetic region, respectively. The spectrum of [Lu(*R*-bbppn)($NO_3$)] corresponds well with that of *R*-bbppn$H_2$, except a broad signal for the hydroxyl protons of free ligand in the lower magnetic field region [33]. All the $^1H$ signals of [Lu(*R*-bbppn)($NO_3$)] are relatively sharp and well-resolved. Such a trend for the complex is consistent with the case of $[Ga(bbpen)]^+$ or $[In(bbpen)]^+$ with a rigid structure in solution [44]. In the dinuclear Zn(II) complex with {Zn(bbpen)} core, on the other hand, the spectral profile is rather

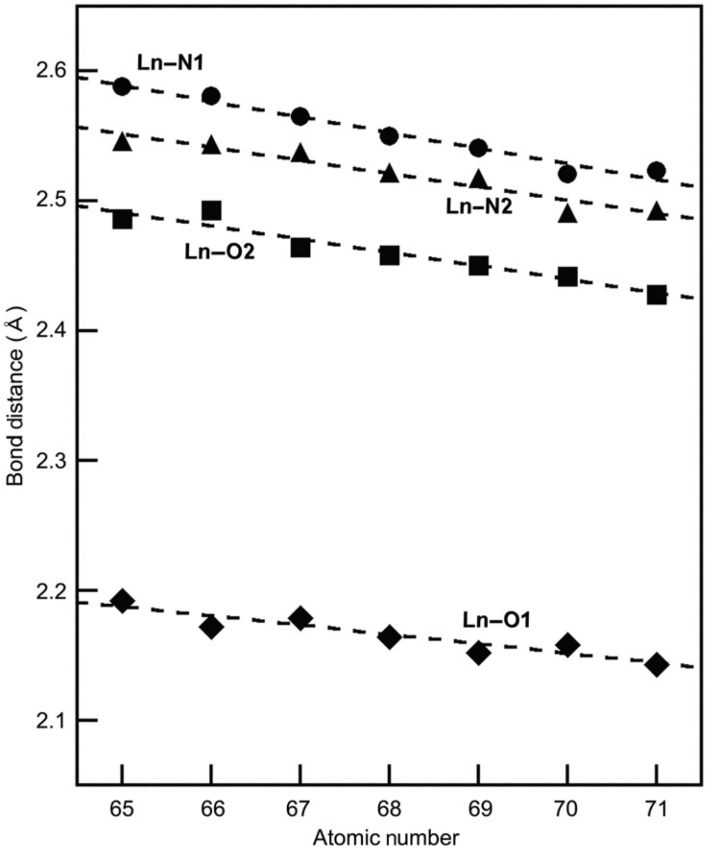

Figure 2. Plots of bond distances against atomic numbers of the complexes.

complicated and accompanied by considerable broadenings [45]. In this case, the {Zn(bbpen)} unit undergoes some conformational change. In contradiction to the Zn(II) complex, no other signals and broadenings were found for [Lu(*R*-bbppn)($NO_3$)]. It seems, therefore, that [Lu(*R*-bbppn)($NO_3$)] retains its rigid structure in $CDCl_3$ without any conformational changes.

The molar conductivities of [Ln(*R*-bbppn)($NO_3$)] in $CH_2Cl_2$ were within the range of 0.03–0.14 $\mathrm{S\,cm^2\,mol^{-1}}$ at 296 K, implying that the complexes exist as neutral species in $CH_2Cl_2$ as well as in the crystalline state. In DMF, on the other hand, all the complexes show significantly larger molar conductivities about 70 $\mathrm{S\,cm^2\,mol^{-1}}$, suggesting that [Ln(*R*-bbppn)($NO_3$)] in DMF undergoes partial dissociation of phenolate or nitrate.

The diffuse reflectance spectrum of [Er(*R*-bbppn)($NO_3$)] is shown in figure 3, as a typical example for the spectra of [Ln(*R*-bbppn)($NO_3$)]. In the crystalline state, [Er(*R*-bbppn)($NO_3$)] has characteristic weak sharp bands for the Er(III) center lower than $30 \times 10^3\,\mathrm{cm^{-1}}$ and intense electronic bands in higher than $30 \times 10^3\,\mathrm{cm^{-1}}$. For the other complexes, the spectral profiles at lower energy depend on the electronic

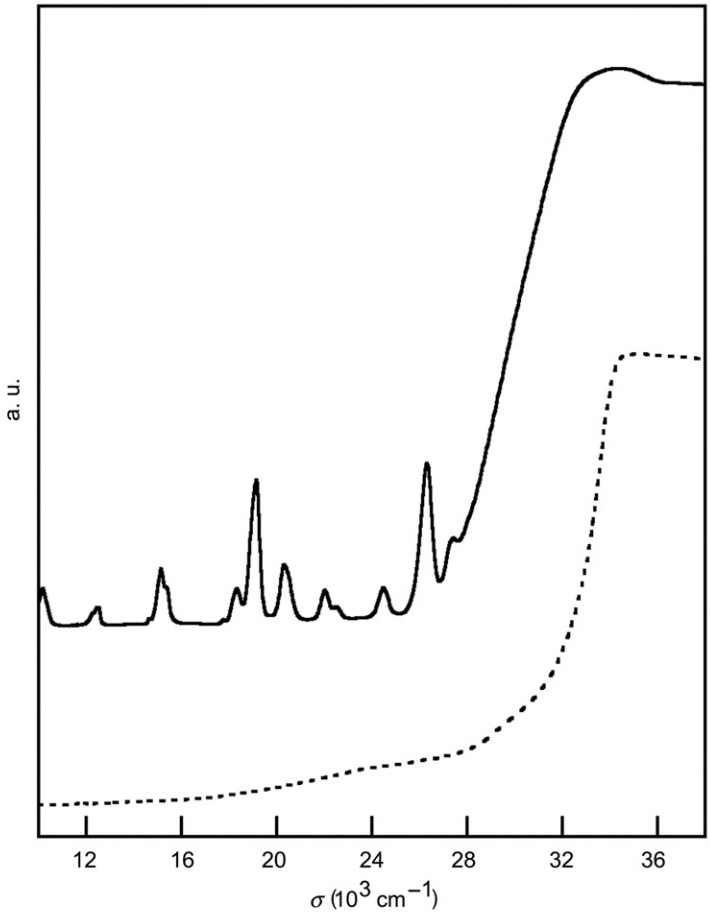

Figure 3. Diffuse reflectance spectra of [Er(*R*-bbppn)($NO_3$)] (solid line) and *R*-bbppn$H_2$ (broken line).

configurations in the f orbitals of Ln(III); the higher energy-side bands are observed at almost the same band positions in the other complexes, and the corresponding bands appear in the spectrum of *R*-bbppn$H_2$. Therefore, these higher energy bands are assigned as localized $\pi$–$\pi^*$ electronic transitions on the ligand *R*-bbppn.

Figure 4 shows the electronic absorption and CD spectra of [Er(*R*-bbppn)($NO_3$)] in $CH_2Cl_2$ together with those in DMF. The spectra of [Er(*R*-bbppn)($NO_3$)] in $CH_2Cl_2$ are essentially consistent with that of diffuse reflection. In $CH_2Cl_2$, more specifically, the corresponding absorption bands to the 12.53, 14.66, 14.7, 15.18, 15.39, 18.2, 18.32, 18.4, 18.5, 19.1, 19.21, 20.28, 20.4, 22.0, 22.10, 22.55, 24.51, 25.7, 26.42, 27.36, 28.0, 33.9, and $40.9 \times 10^3\,\mathrm{cm}^{-1}$ bands in the reflectance spectra appear at 12.54, 14.9, 15.1, 15.18, 15.40, 18.2, 18.32, 18.42, 18.6, 19.2, 19.21, 20.31, 20.4, 22.0, 22.12, 22.60, 24.54, 25.5, 26.42, 27.40, 28.1, 34.4, and $41.49 \times 10^3\,\mathrm{cm}^{-1}$, respectively. Similar trends are also observed for the other complexes, [Ln(*R*-bbppn)($NO_3$)] (Ln = Tb, Dy, Ho, Tm,

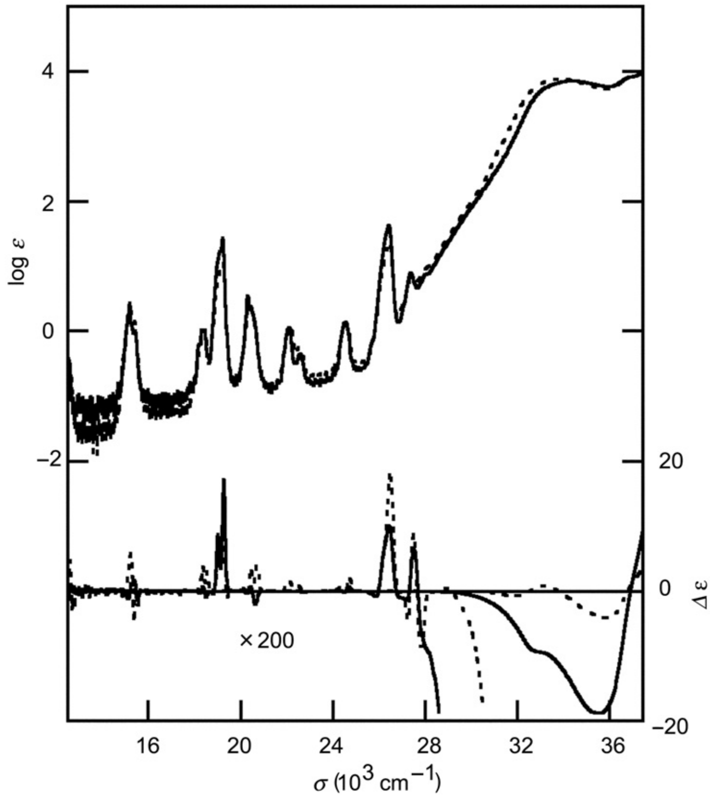

Figure 4. Electronic absorption and CD spectra of [Er(*R*-bbppn)(NO$_3$)] in CH$_2$Cl$_2$ (solid line) and DMF (broken line).

Yb, Lu). These imply that the complexes retain their structure in CH$_2$Cl$_2$, as in the solid state. The stable structures of the complexes are also supported by the molar conductivities in CH$_2$Cl$_2$ and $^1$H NMR spectrum in CDCl$_3$ for [Lu(*R*-bbppn)(NO$_3$)]. In CH$_2$Cl$_2$, [Er(*R*-bbppn)(NO$_3$)] exhibits weak sharp CD signals lower than $30 \times 10^3\,\mathrm{cm}^{-1}$ and intense CD signals at higher energy. The latter higher energy CD bands of [Er(*R*-bbppn)(NO$_3$)] are also observed at the same band positions with the same intensities in the other Ln(III) complexes. Although *R*-bbppnH$_2$ exhibits a similar CD spectral behavior to [Ln(*R*-bbppn)(NO$_3$)] in the higher energy side than $30 \times 10^3\,\mathrm{cm}^{-1}$, the intensity of each band is weaker than that of the corresponding band in [Ln(*R*-bbppn)(NO$_3$)] (figure 5). This implies that the rigid polyhedral formation by complexation with Ln(III) induces a chiral amplification of $\pi$-electronic system of the ligand. No significant differences in the absorption spectra of [Er(*R*-bbppn)(NO$_3$)] can be recognized between CH$_2$Cl$_2$ and DMF, indicating that the partial dissociation of ligand in DMF is due not to *R*-bbppn but to NO$_3^-$.

Tb(III) complexes have attracted the attention as green-light emitting devices [46, 47]. The present Tb(III) complex, [Tb(*R*-bbppn)(NO$_3$)], also is an yellowish-green light emitter on exposure to ultraviolet light. The photoluminescence spectrum of

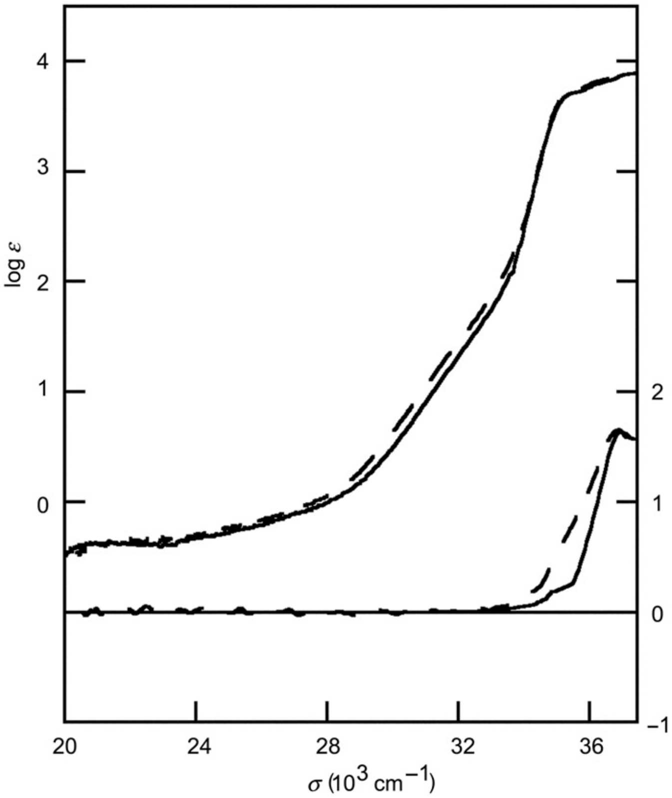

Figure 5. Electronic absorption and CD spectra of *R*-bbppn$H_2$ in $CH_2Cl_2$ (solid line) and DMF (broken line).

[Tb(*R*-bbppn)($NO_3$)] in solid state at room temperature is composed of several sharp bands in the 450–700 nm region (figure 6). These luminescent transitions arise from the $^5D_4$ level to the ground state manifold $^7F_J$ ($J = 0$–6) [48, 49]. The most intense band at 550.0 nm is assigned as $^5D_4 \rightarrow {}^7F_5$ transition, corresponding to the green emission [48, 49]. This implies that [Tb(*R*-bbppn)($NO_3$)] has potential as a green-light emitting device.

## Supplementary material

CCDC-702155 for [Tb(*R*-bbppn)($NO_3$)], CCDC-702156 for [Dy(*R*-bbppn)($NO_3$)], CCDC-702157 for [Ho(*R*-bbppn)($NO_3$)], CCDC-702158 for [Er(*R*-bbppn)($NO_3$)], CCDC-702159 for [Tm(*R*-bbppn)($NO_3$)], CCDC-702160 for [Yb(*R*-bbppn)($NO_3$)], and CCDC-702161 for [Lu(*R*-bbppn)($NO_3$)] contain the supplementary crystallographic data for this article. These data can be obtained free of charge at www.ccdc.cam.ac.uk/conts/retrieving.html [or from the Cambridge Crystallographic

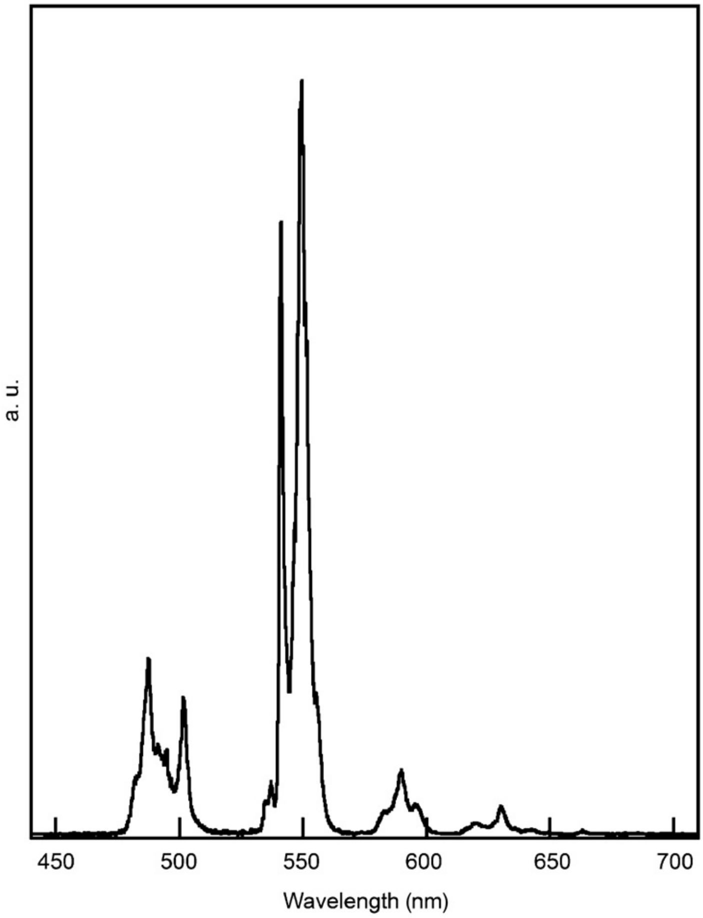

Figure 6. Photoluminescence spectrum of [Tb(*R*-bbppn)($NO_3$)] in solid state at room temperature.

Data Centre, 12 Union Road, Cambridge CB2 1EZ, UK; Fax: +44 1223 336 033; E-mail: deposit@ccdc.cam.ac.jk].

## Acknowledgments

This work was partly supported by Grants-in-Aid for Scientific Research from the Ministry of Education, Culture, Sports, Science, and Technology.

## References

[1] Y. Saito. *Coord. Chem. Rev.*, **13**, 305 (1974).
[2] S. Kirschner, I. Bakkar. *Coord. Chem. Rev.*, **43**, 325 (1982).
[3] Y. Yamada, Y. Maeda, Y. Miyashita, K. Fujisawa, T. Konno, K. Okamoto. *Bull. Chem. Soc. Jpn.*, **73**, 1219 (2000).

[4] Y. Yamada, Y. Maeda, K. Fujisawa, T. Konno, K. Okamoto. *Bull. Chem. Soc. Jpn.*, **73**, 1831 (2000).

[5] Y. Yamada, Y. Miyashita, K. Fujisawa, K. Okamoto. *Bull. Chem. Soc. Jpn.*, **75**, 1151 (2002).

[6] Y. Yamada, M. Uchida, M. Fujita, Y. Miyashita, K. Okamoto. *Polyhedron*, **22**, 1507 (2003).

[7] Y. Yamada, M. Noda, M. Inoue, Y. Miyashita, K. Okamoto, M. Koikawa, T. Tokii. *J. Coord. Chem.*, **60**, 607 (2007).

[8] T.A. Beineke, J. Delgaudio. *Inorg. Chem.*, **7**, 715 (1968).

[9] A. Zalkin, D.H. Templeton, D.G. Karraker. *Inorg. Chem.*, **8**, 2680 (1969).

[10] T.J. Anderson, M.A. Neuman, G.A. Melson. *Inorg. Chem.*, **12**, 927 (1973).

[11] L.F. Lindoy. *Coord. Chem. Rev.*, **48**, 83 (1976).

[12] R.C. Mehrotra, P.N. Kapoor, J.M. Batwara. *Coord. Chem. Rev.*, **31**, 67 (1980).

[13] Y. Ohki, Y. Suzuki, M. Shimoi, A. Ouchi. *Bull. Chem. Soc. Jpn.*, **59**, 1015 (1986).

[14] Y. Sugita, A. Ouchi. *Bull. Chem. Soc. Jpn.*, **60**, 171 (1987).

[15] Y. Ohki, Y. Suzuki, M. Shimoi, A. Ouchi. *Bull. Chem. Soc. Jpn.*, **60**, 551 (1987).

[16] Y. Ohki, Y. Suzuki, A. Ouchi. *Bull. Chem. Soc. Jpn.*, **60**, 1543 (1987).

[17] Y. Tateyama, Y. Ohki, Y. Suzuki, A. Ouchi. *Bull. Chem. Soc. Jpn.*, **61**, 2214 (1988).

[18] Y. Tateyama, Y. Kuniyasu, Y. Suzuki, A. Ouchi. *Bull. Chem. Soc. Jpn.*, **61**, 2805 (1988).

[19] A. Ouchi, Y. Suzuki, Y. Ohki, Y. Koizumi. *Coord. Chem. Rev.*, **92**, 29 (1988).

[20] N. Sabbatini, M. Guardigli, J. Lehn. *Coord. Chem. Rev.*, **123**, 201 (1993).

[21] R. Baggio, M.T. Garland, M. Perec. *Inorg. Chem.*, **36**, 950 (1997).

[22] L. Thunus, R. Lejeune. *Coord. Chem. Rev.*, **184**, 1 (1999).

[23] D. Parker. *Coord. Chem. Rev.*, **205**, 109 (2000).

[24] H. Tsukube, S. Shinoda, H. Tamiaki. *Coord. Chem. Rev.*, **226**, 227 (2002).

[25] Z. Hou, Y. Wakatsuki. *Coord. Chem. Rev.*, **231**, 1 (2002).

[26] G. Malandrino, I.L. Fragalà. *Coord. Chem. Rev.*, **250**, 1605 (2006).

[27] R.C. Evans, P. Douglas, C.J. Winscom. *Coord. Chem. Rev.*, **250**, 2093 (2006).

[28] S. Tanase, J. Reedijk. *Coord. Chem. Rev.*, **250**, 2501 (2006).

[29] I.A. Setyawati, S. Liu, S.J. Rettig, C. Orvig. *Inorg. Chem.*, **39**, 496 (2000).

[30] D.L. Kepert. *J. Chem. Soc.*, 4736 (1965).

[31] D.G. Blight, D.L. Kepert. *Theor. Chim. Acta*, **11**, 51 (1968).

[32] D.G. Blight, D.L. Kepert. *Inorg. Chem.*, **11**, 1556 (1972).

[33] Anal. Calc. for $C_{29}H_{32}N_4O_2$ (R-bbppnH$_2$): C, 74.33; H, 6.88; N, 11.96%. Found: C, 74.32; H, 6.89; N, 11.91%. UV-Vis spectrum in $CH_2Cl_2$ [$\nu_{max}$, $10^3$ cm$^{-1}$ (log $\epsilon$/mol$^{-1}$ dm$^3$ cm$^{-1}$)]: 35.7 (3.7)sh, 37.3 (3.9)sh, 38.0 (3.9)sh. UV-Vis spectrum in DMF [$\nu_{max}$, $10^3$ cm$^{-1}$ (log $\epsilon$/mol$^{-1}$ dm$^3$ cm$^{-1}$)]: 35.2 (3.7)sh, 36.2 (3.8)sh. CD spectrum in $CH_2Cl_2$ [$\nu_{max}$, $10^3$ cm$^{-1}$ ($\Delta\epsilon$)]: 36.97 (1.64), 37.5 (1.6)sh, 38.99 (1.13), 39.8 (1.0)sh, 40.65 (1.13), 41.5 (1.3)sh, 42.19 (1.36), 42.82 (1.27), 43.38 (1.13). CD spectrum in DMF [$\nu_{max}$, $10^3$ cm$^{-1}$ ($\Delta\epsilon$)]: 36.90 (1.66). $^1$H NMR (300 MHz, $CDCl_3$), $\delta = 0.97$ (d, 3H, methyl), 2.46 (dd, 1H, methylene), 2.79 (dd, 1H, methylene), 3.17 (td, 1H, methine), 3.55–3.93 (m, 8H, methylene), 6.65–6.89 (m, 6H, phenyl), 7.03–7.18 (m, 6H, ring), 7.58–7.64 (m, 2H, pyridyl), 8.56 (t, 2H, pyridyl), 10.98 (brs, 2H, hydroxyl).

[34] Landoldt-Börnstein. *Neue Serie II/11*, Springer-Verlag, Berlin (1981).

[35] F. Hai-Fu. *SAPI91, Structure Analysis Programs with Intelligent Control*, Rigaku Corporation, Tokyo, Japan (1991).

[36] P.T. Beurskens, G. Admiraal, G. Beurskens, W.P. Bosman, R. de Gelder, R. Israel, J.M.M. Smits. *DIRDIF99*, *The DIRDIF 99 Program System*, Technical Report of the Crystallography Laboratory, University of Nijmegen, The Netherlands (1994).

[37] D.T. Cromer, J.T. Waber (Eds.). *International Tables for X-ray Crystallography*, Vol. IV, The Kynoch Press, Birmingham, England, Table 2.2 A (1974).

[38] J.A. Ibers, W.C. Hamilton. *Acta Cryst.*, **17**, 781 (1964).

[39] D.C. Creagh, W.J. McAuley. In *International Tables for Crystallography*, A.J.C. Wilson (Ed.), Vol. C, pp. 219–222, Kluwer Academic Publishers, Boston (1992).

[40] D.C. Creagh, J.H. Hubbell. In *International Tables for Crystallography*, A.J.C. Wilson (Ed.), Vol. C, pp. 200–206, Kluwer Academic Publishers, Boston (1992).

[41] H.D. Flack. *Acta Cryst.*, **A39**, 876 (1983).

[42] *teXsan 1.9: Crystal Structure Analysis Package*, Molecular Structure Corporation, 9009 New Trails Dr., The Woodlands, TX 77381, USA (1998).

[43] M. Brorson, T. Damhus, C.E. Schaeffer. *Inorg. Chem.*, **22**, 1569 (1983).

[44] E. Wong, S. Liu, S.J. Rettig, C. Orvig. *Inorg. Chem.*, **34**, 3057 (1995).

[45] H. Adams, D. Bradshaw, D.E. Fenton. *Eur. J. Inorg. Chem.*, 859 (2001).

[46] D. Parker, J.A.G. Williams. *Dalton Trans.*, 3613 (1996).

[47] J. Kido, Y. Okamoto. *Chem. Rev.*, **102**, 2357 (2002).

[48] E. Kusrini, M.I. Saleh. *Inorg. Chim. Acta*, **362**, 4025 (2009).

[49] E.S. Andreiadis, R. Demadrille, D. Imbert, J.P. Caut, M. Mazzanti. *Chem. Eur. J.*, **15**, 9458 (2009).